Improved quality $(11\bar{2}0)$ *a*-plane GaN with sidewall lateral epitaxial overgrowth

Bilge M. Imer,[a] Feng Wu, Steven P. DenBaars, and James S. Speck
Materials Department and NICP ERATO/JST Group, University of California, Santa Barbara, California 93106

(Received 7 October 2005; accepted 28 December 2005; published online 7 February 2006)

We demonstrate a technique to reduce the extended defect densities in *a*-plane GaN deposited on *r*-plane sapphire. The SiO_2 lateral epitaxial overgrowth mask consisted of $\langle 1\bar{1}00\rangle_{GaN}$ stripes. Both the mask and GaN were etched through the mask openings and the lateral growth was initiated from the etched *c*-plane GaN sidewalls, and the material was grown over the mask regions until a smooth coalesced film was achieved. Threading dislocation densities in the range of 10^6–10^7 cm^{-2} were realized throughout the film surface. The on-axis and off-axis full width at half maximum value and surface roughness were 0.082°, 0.114°, and 0.622 nm, respectively. © *2006 American Institute of Physics*. [DOI: 10.1063/1.2172159]

The presence of polarization-related internal electric fields hinders the performance of III-nitride devices. The spontaneous and piezoelectric polarizations which are parallel to [0001] *c* direction are caused by the composition and strain, respectively. The polarization-related electric fields cause electron and hole separation in quantum wells which lead to poor recombination efficiencies, reduced oscillator strength, and redshift in emission wavelength. To avoid such polarization effects, growth along nonpolar orientations has been explored for planar *a*-plane GaN on *r*-plane sapphire[1] and *a*-plane SiC[2] with metalorganic chemical vapor deposition (MOCVD), and with hydride vapor phase epitaxy (HVPE),[3] and planar *m*-plane GaN with molecular beam epitaxy[4,5] and HVPE.[6] The recent studies of *a*-plane[7,8] and *m*-plane[9,10] AlGaN/GaN quantum wells and *a*-plane[11,12] and *m*-plane[13] GaN/InGaN quantum wells demonstrate that it is possible to eliminate such polarization fields by growing device structures along these nonpolar orientations.

Another obstacle, which is as important to address and solve, is the presence of extended defects, such as stacking faults and threading dislocations, in current state-of-the-art nonpolar GaN films. MOCVD grown *a*-plane GaN on *r*-plane Al_2O_3 has a threading dislocation (TD) density of $\sim 3\times 10^{10}$ cm^{-2} and a basal stacking fault density of $\sim 3.5\times 10^5$ cm^{-1}.[1] The threading dislocations (TDs) in GaN act as nonradiative recombination centers, and charge scattering centers for carriers causing low mobilities. TDs are also associated with leakage current in *p*-*n* junctions.[14] Therefore reducing, ideally completely eliminating, these extended defects is essential to improve device performance.

To reduce extended defect densities, mainly TDs in (0001) oriented polar GaN and TDs and stacking faults in nonpolar oriented GaN, many methods have been studied over the years. For polar *c*-plane GaN some of these methods include: single-step lateral epitaxial overgrowth (LEO);[15] air-bridged LEO;[16] facet controlled LEO;[17] cantilever epitaxy;[18] and pendeoepitaxy[19,20] where the SiC substrate is used as a *pseudomask*. The methods used to reduce defects for nonpolar GaN include: single-step LEO;[21] and selective area LEO[22] which is similar to two-step LEO. With the single-step LEO technique for nonpolar GaN,[21] $\langle 1\bar{1}00\rangle_{GaN}$ oriented stripes have yielded the best quality material creating vertical *c*-plane Ga-face and N-face sidewalls, because the TDs were confined under the mask region and were present only in the seed region extending to the surface parallel to the growth direction. The stacking faults on the basal plane were associated with growth on exposed $(000\bar{1})$ N faces. The N-face growth rate was an order of magnitude slower than Ga-face growth which limited the presence of basal stacking faults. We will be demonstrating a technique, sidewall lateral epitaxial overgrowth (SLEO), to reduce the defect densities in both window and wing regions as effectively as a double-step LEO with the simplicity of the single-step LEO process.

The *a*-plane GaN templates were grown with low pressure MOCVD on double side polished *r*-plane Al_2O_3 substrates using conditions described in Ref. 1. The SiO_2 mask was deposited over the *a*-plane GaN templates using plasma enhanced chemical vapor deposition. A 2 μm/8 μm (window/wing) LEO stripe pattern was used for 3 μm *a*-plane GaN template and 5 μm/15 μm LEO stripes were patterned over 6 μm *a*-plane GaN template. The mask pattern was transferred by using conventional photolithography techniques. The stripe orientation was chosen parallel to the $\langle 1\bar{1}00\rangle_{GaN}$ direction to realize vertical *c*-plane sidewalls.[21] Mask patterning was followed by etching of SiO_2 using inductively coupled plasma etching through the windows to the GaN epitaxial film. Finally, reactive ion etching was used for GaN etching through the mask openings, not necessarily down to the *r*-plane sapphire substrate, thus exposing Ga-face (0001) and N-face $(000\bar{1})$ planes on the sidewalls and $(11\bar{2}0)$ plane at the bottom of the trenches. The etch depth was chosen such that it was greater than the window width so that there was sufficient space for the material to grow laterally from the sidewalls. Figure 1(a) schematically shows the main processing steps. After etching the nitride, the sample was loaded into reactor for regrowth. Atomic force microscopy (AFM) images were captured by Digital Instruments D3000 in tapping mode. The mosaic of the films was determined by using Philips MRD PRO in

[a]Electronic mail: bilge@engineering.ucsb.edu

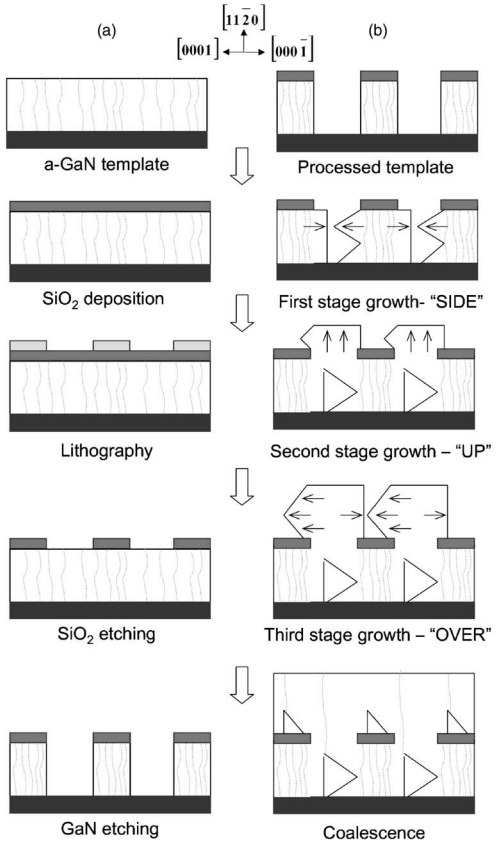

FIG. 1. (a) Processing sequence of the *a*-GaN template for subsequent sidewall lateral overgrowth. (b) Schematic of the growth stages of sidewall lateral epitaxial overgrowth (SLEO).

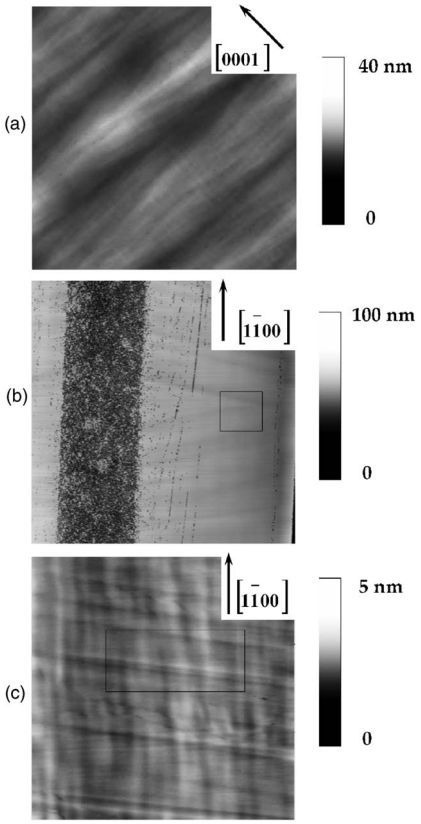

FIG. 2. Atomic force microscopy (AFM) images of *a*-GaN: (a) planar *a*-GaN (6 nm rms); (b) 5 μm/15 μm (window/wing) stripes single-step LEO *a*-GaN (5.82 nm rms); (c) 5 μm/15 μm (window/wing) stripes sidewall LEO *a*-GaN (0.62 nm rms).

receiving slit (rocking curve) mode. Transmission electron microscopy (TEM) characterization was carried out with FEI Tecnia G2 Sphera Microscope at an operating voltage of 200 kV. Scanning electron microscopy (SEM) images were recorded with an FEI Sirion and FEOL 6300 FE-SEM instruments. Cathodoluminescence (CL) images were obtained at room temperature with an operating voltage of 5 kV using a Gatan MonoCL system.

During GaN SLEO there were three main stages of growth of interest as shown in Fig. 1(b). The first, "SIDE," stage involved growth predominantly from the exposed Ga-face sidewall until coalescence with the opposite N-face sidewall—this stage suppressed growth from the bottom of the trench by starving the bottom of precursor species. The N face formed straight sidewalls with hexagonal hillock features, and the Ga-face grew ~10 times faster than the N-face confining the stacking faults only to these slow growing N-face regions. The Ga-face sidewall formed an arrowhead shape with inclined $\{11\bar{2}n\}$ facets. The high lateral growth rates of the Ga face were favored by high growth temperatures, ~1190 °C, low pressure and low V/III ratio, ~700–800. Both the second, "UP," growth mode and the third, "OVER," growth mode required high temperature, low pressure growth and concurrently progressively decreasing V/III ratio from ~700–800 to ~300, as the material coalesced and formed a continuous film. For all three stages, high lateral to vertical growth rate ratios were preferred.

The AFM images in Fig. 2 demonstrate the improvement in film quality of fully coalesced *a*-plane GaN by utilizing SLEO. In Fig. 2(b), it is possible to see the surface quality contrast between the wing and the window regions for single step LEO. While in window regions, where the threading dislocations were still present and were associated with surface depression,[21] the rms values were comparable with planar *a*-plane GaN; in overgrown wing regions the surface quality was comparable with the SLEO film. The surface roughness for the whole SLEO film surface improved, Fig. 2(c); it was as low as the wing region of the single-step LEO film, Fig. 2(b). Table I gives a comparison in between planar, single-step LEO for 5 μm/15 μm (window/wing) stripes, and SLEO films for 5 μm/15 μm (window/wing) stripes in terms of surface roughness values, crystal quality full width at half maximum (FWHM) values for on- and off-axis x-ray rocking curve, and threading dislocation densities determined by plan-view TEM. With the SLEO technique, the surface roughness values were improved by one order of magnitude with a rms value of ~6 Å. The on- and off-axis FWHM values were decreased by a factor of 4 with respect to planar *a*-GaN yielding a value even comparable with single-step LEO *c*-plane GaN crystal quality. TEM results show that the TD densities were in the range of 10^6–10^7 cm^{-2}, three to four orders of magnitude lower than planar films, and the stacking fault densities were in the range of 10^3–10^4 cm^{-1}, one to two orders of magnitude lower than planar *a*-GaN films depending on the stripe size. For wider wing and/or window stripe size the stacking fault densities were lower due to high Ga-face growth over N face.

Figure 3(a) is a cross-sectional SEM image of a coalesced SLEO *a*-plane GaN with 2 μm/8 μm (window / wing) stripes. The coalescence was achieved in the early

TABLE I. Surface roughness from AFM images, x-ray rocking curve widths and threading dislocation density for: planar *a*-GaN, single step LEO *a*-GaN (5 μm/15 μm window/wing stripes), and SLEO *a*-GaN.

	Surface roughness rms	X-ray rocking curve FWHM		TD density
		On axis $(11\bar{2}0)$	Off axis $(10\bar{1}1)$	
Planar *a*-GaN	6.0 nm	0.29°	0.46°	$\sim 10^{10}$ cm^{-2} throughout the material
Single step LEO *a*-GaN	5.82 nm	0.17°	0.27°	$\sim 10^{7}$–10^{8} cm^{-2} only in the wing region
Sidewall LEO *a*-GaN	0.62 nm	0.082°	0.114°	$\sim 10^{6}$–10^{7} cm^{-2} throughout the material

stages. This promises, with the same growth conditions, it is possible to coalesce wider stripes. With the presence of defected seed regions, such as the window region in single-step LEO, the film coalescence was almost impossible to achieve, and the yield and reproducibility was an issue with MOCVD. We speculate that the absence of TDs in the seed regions facilitated homogeneous growth leading to coalescence with the proper growth conditions.

When continuous *a*-plane SLEO material was achieved, there were two coalescence fronts. Each coalescence front was associated with a planar array of TDs, as can be seen from Fig. 3(b) which shows the CL emission across the SLEO film; there was one single dislocation line propagating to the surface at each coalescence front. A recent study done by Haskell *et al.*[23] showed that stacking faults do not act as nonradiative recombination centers in nonpolar III-nitrides. So the dark regions in CL image, Fig 3(b), are associated with TDs at the coalescence fronts and TDs that bound stacking faults rather than being solely stacking faults.

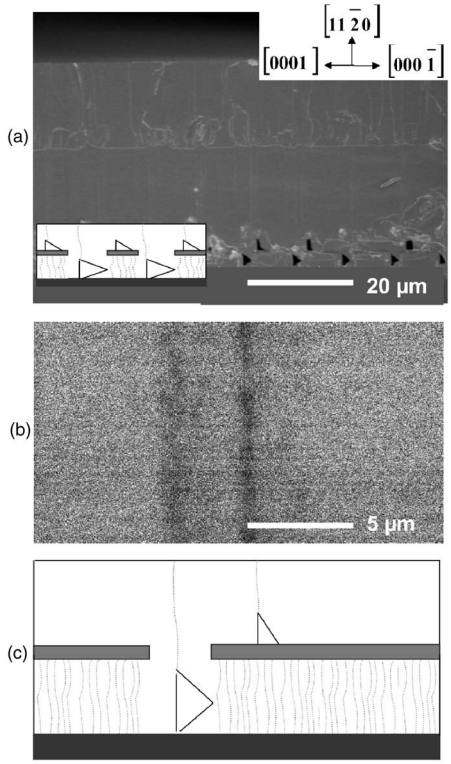

FIG. 3. (a) Cross-sectional SEM of the coalesced SLEO *a*-plane GaN film with 2 μm/8 μm (window/wing) stripes. (b) Panchromatic CL image of the top surface of the coalesced SLEO *a*-plane GaN film. (c) Schematic cross section of the coalesced SLEO *a*-plane GaN film showing the coalescence fronts.

The authors would like to acknowledge the support of JST/ERATO and the National Science Foundation for use of facilities through the MRSEC program.

[1] M. D. Craven, S. H. Lim, F. Wu, J. S. Speck, and S. P. DenBaars, Appl. Phys. Lett. **81**, 469 (2002).
[2] M. D. Craven, A. Chakraborty, B. Imer, F. Wu, S. Keller, U. K. Mishra, J. S. Speck, and S. P. DenBaars, Phys. Status Solidi C **1**, 4 (2003).
[3] B. A. Haskell, F. Wu, S. Matsuda, M. D. Craven, P. T. Fini, S. P. DenBaars, J. S. Speck, and S. Nakamura, Appl. Phys. Lett. **83**, 1554 (2003).
[4] E. S. Hellman, Z. Liliental-Weber, and D. N. E. Buchanan, MRS Internet J. Nitride Semicond. Res. **2**, 30 (1997).
[5] P. Waltereit, O. Brandt, M. Ramsteiner, A. Trampert, H. T. Grahn, J. Menniger, M. Reiche, R. Uecker, P. Reiche, and K. H. Ploog, Phys. Status Solidi A **180**, 133 (2000).
[6] B. A. Haskell, A. Chakraborty, F. Wu, H. Sasano, P. T. Fini, S. P. Denbaars, J. S. Speck, and S. Nakamura, J. Electron. Mater. **34**, 357 (2005).
[7] G. A. Garrett, H. Shen, M. Wraback, B. Imer, B. Haskell, J. S. Speck, S. Keller, S. Nakamura, and S. P. DenBaars, Phys. Status Solidi A **202**, 846 (2005).
[8] H. M. Ng, Appl. Phys. Lett. **80**, 4369 (2002).
[9] P. Waltereit, O. Brandt, A. Trampert, H. T. Grahn, J. Menniger, M. Ramsteiner, M. Reiche, and K. H. Ploog, Nature (London) **406**, 865 (2000).
[10] A. Bhattacharya, I. Friel, S. Iyer, T.-C. Chen, W. Li, J. Cabalu, Y. Fedyunin, K. F. Ludwig, Jr., T. D. Moustakas, H.-P. Maruska, D. W. Hill, J. J. Gallagher, M. C. Chou, and B. Chai, J. Cryst. Growth **251**, 487 (2003).
[11] A. Chakraborty, B. A. Haskell, S. Keller, J. S. Speck, S. P. DenBaars, S. Nakamura, and U. K. Mishra, Appl. Phys. Lett. **85**, 5143 (2004).
[12] A. Chakraborty, S. Keller, C. Meier, B. A. Haskell, S. Keller, P. Waltereit, S. P. DenBaars, S. Nakamura, J. S. Speck, and U. K. Mishra, Appl. Phys. Lett. **86**, 031901 (2005).
[13] A. Chakraborty, B. A. Haskell, S. Keller, J. S. Speck, S. P. DenBaars, S. Nakamura, and U. K. Mishra, Jpn. J. Appl. Phys., Part 2 **44**, L173 (2005).
[14] J. S. Speck and S. J. Rosner, Physica B, **273–274**, 24 (1999).
[15] P. Fini, L. Zhao, B. Moran, M. Hansen, H. Marchand, J. P. Ibbetson, S. P. DenBaars, U. K. Mishra, and J. S. Speck, Appl. Phys. Lett. **75**, 1706 (1999).
[16] I. Kidoguchi, A. Ishibashi, G. Sugahara, and Y. Ban, Appl. Phys. Lett. **76**, 3768 (2000).
[17] K. Hiramatsu, K. Nishiyama, M. Onishi, H. Mizutani, M. Narukawa, A. Motogaito, H. Miyake, Y. Iyechika, and T. Maeda, J. Cryst. Growth **221**, 316 (2000).
[18] C. I. H. Ashby, C. C. Mitchell, J. Han, N. A. Missert, P. P. Provencio, D. M. Follstaedt, G. M. Peake, and L. Griego, Appl. Phys. Lett. **77**, 3233 (2000).
[19] K. Linthicum, T. Gehrke, D. Thomson, E. Carlson, P. Rajagopal, T. Smith, D. Batchelor, and R. Davis, Appl. Phys. Lett. **75**, 196 (1999).
[20] T. S. Zheleva, W. M. Ashmawi, and K. A. Jones, Phys. Status Solidi A **176**, 545 (1999).
[21] M. D. Craven, S. H. Lim, F. Wu, J. S. Speck, and S. P. DenBaars, Appl. Phys. Lett. **81**, 1201 (2002).
[22] C. Chen, J. Zhang, J. Yang, V. Adivarhan, S. Rai, S. Wu, H. Wang, W. Sun, M. Su, Z. Gong, E. Kuokstis, M. Gaevski, and M. A. Khan, Jpn. J. Appl. Phys., Part 2 **42**, L818 (2003).
[23] B. A. Haskell, T. J. Baker, M. B. McLaurin, F. Wu, P. T. Fini, S. P. DenBaars, J. S. Speck, and S. Nakamura, Appl. Phys. Lett. **86**, 111917 (2005).